Available online at www.sciencedirect.com

ScienceDirect

Thermochimica Acta 459 (2007) 26–33

thermochimica acta

www.elsevier.com/locate/tca

Thermal decomposition kinetics of a mixture of energetic polymer and nitramine oxidizer

Sreekumar Pisharath*, How Ghee Ang

Energetic Materials Research Centre, Nanyang Technological University, 50 Nanyang Avenue, Singapore 639798, Singapore

Received 30 August 2006; received in revised form 20 March 2007; accepted 20 March 2007
Available online 30 March 2007

Abstract

Energetic glycidyl azide polymer (GAP) was synthesized from polyepichlorohydrin (PECH) precursor. Thermal decomposition behavior of a mixture of GAP and nitramine oxidizer (4,10-dinitro-2,6,8,12-tetraoxa-4,10-diazaisowurtzitane (TEX)) was investigated by using thermogravimetric analysis (TGA) and differential scanning calorimetry (DSC). It was found that the decomposition temperature of TEX is unaffected by the presence of GAP in the GAP/TEX mixture. Kinetics of degradation of GAP/TEX mixture was studied by a model-free method and the results were compared with that of the pure components. The study suggested that the decomposition kinetics is controlled by the degradation of GAP during the initial stages of conversion ($\alpha > 0.25$) whereas the later stages ($0.25 \leq \alpha \leq 1$) are determined by that of TEX. Mechanistic interpretation has been provided to the observed activation energy dependencies by using a combination of optical microscopy (OM) and Fourier transform infrared spectroscopy (FTIR).

Keywords: Thermal decomposition kinetics; Energetic polymer; Model-free method

1. Introduction

Thermal analysis is an integral part of research and development of energetic materials (EM) [1]. The physio-chemical processes that occur during the thermolysis of (EM) control their performance. It also provides a relative measure of their thermal stability. Thus investigation of thermal decomposition kinetics of EMs is important for their performance prediction and safety evaluation. EMs when they are applied as propellant formulations or polymer bonded explosives (PBX), are usually compounded with other components such as polymer binders, plasticizers, and burn rate enhancers. Presence of binders significantly influences the thermochemistry of EM.

In this paper, we investigate the thermal decomposition characteristics of high performance nitramine oxidizer 4,10-dinitro-2,6,8,12-tetraoxa-4,10-diazaisowurtzitane (TEX), with an energetic glycidyl azide polymer (GAP). Themogravimetric analysis (TGA) was adopted to study the thermal decomposition characteristics.

GAP is widely studied among the energetic azido polymers as a binder in rocket propellants. It is characterized by the presence of C–N_3 (azido) group attached to the polymer backbone. Each azide group contributes 378 kJ of energy to polymer molecule providing an overall positive heat of formation of +0.96 kJ/g. The exothermic decomposition of the azide group releasing enormous energy provides high burn rate to GAP based formulations. Moreover, the fuel-rich composition of GAP reduces the molecular weight of the exhaust gases, increasing the specific impulse [2–4].

There is currently considerable interest on the use of high density nitramine oxidizers in gun and rocket propellants due to their desirable properties, such as, absence of noxious combustion products, high specific impulse and impetus, and thermal stability. TEX is a high density nitramine oxidizer with high detonation velocity and low sensitivity towards friction and impact [5]. However, nitramine oxidizers suffer from low burn rate characteristics, high pressure rate exponents, and very high flame temperatures (3000 K). Hence GAP binders are mixed with nitramine oxidizers to produce propellant formulations with high thermal stability, improved burn rates, and low flame temperatures [6].

The important objective of thermolysis experiments is to obtain kinetic parameters, i.e. activation energy and pre-

---

* Corresponding author. Tel.: +65 67906409; fax: +65 67927173.
E-mail address: sreekumar@ntu.edu.sg (S. Pisharath).

0040-6031/$ – see front matter
doi:10.1016/j.tca.2007.03.017

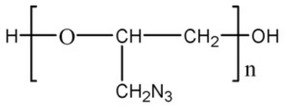

$$\mathrm{H}\left[\mathrm{O-\underset{\displaystyle CH_2N_3}{\underset{|}{CH}}-CH_2}\right]_n\mathrm{OH}$$

Glycidyl Azide Polymer (GAP)

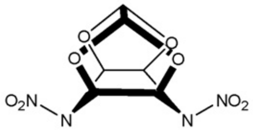

4, 10-dinitro-2, 6, 8, 12-tetraoxa-4, 10-diazaisowurtzitane (TEX)

Fig. 1. Chemical structures of GAP and TEX.

exponential factor that depict the thermal decomposition process. These kinetic parameters could be utilized for safety evaluation and performance prediction of EMs. For example, Zeman [7] correlated the activation energy of thermal decomposition of explosives with detonation rate by a modified Evans–Polanyi–Semenov equation. Similar correlations of Arrhenius parameters could also be obtained with heat of explosion, molecular structure, and detonation characteristics; namely detonation velocity, Chapman–Jouguet pressure, and detonation energy [8,9]. Hence it is important to obtain reliable kinetic data out of thermal decomposition experiments.

Model-fitting methods, employing single heating rates are widely used for obtaining global activation energy and pre-exponential factor from thermolysis experiments. This method provides single values of activation energy for the overall process. However, the majority of the thermal decomposition processes of EMs involve multiple step reactions with variable activation energies and reaction mechanisms. The values obtained from the model-fitting methods are average, which do not reflect changes in reaction mechanism and kinetics with respect to temperature and extent of decomposition [10,11].

Model-free (isoconversional) methods allow the determination of activation energy as a function of extent of decomposition and temperature. This dependence is determined without making any implicit assumptions on the reaction model. The behavior of the material could be reliably predicted by determining the dependence of activation energy on conversion. Model-free kinetics are widely used to study the kinetics of a variety of physical processes [12–14].

Herein, we explore the advantages of model-free method to understand the decomposition kinetics of TEX in the presence of the energetic polymer GAP. Fig. 1 presents the chemical structures of GAP and TEX. In the study, a mixture of TEX and uncured GAP was used which could be referred to as a pseudo-propellant.

2. Experimental

2.1. Materials

Epichlorohydrin (ECH) obtained from Acros Organics with 99% purity, BF_3-dimethyl ether complex obtained from Merck and 1,4,butanediol (BDO) obtained from Fluka were used as-received. Methylene chloride and dimethyl formamide (DMF) obtained from JT-Baker, were distilled under reduced pressure and stored over molecular sieves.

2.2. Methods

GAP polymer was synthesized in two steps. Scheme 1 outlines the synthesis of GAP. First step was the synthesis of poly(epichlorohydrin) (PECH) of adequate molecular weight. The second step was, conversion of PECH polymer to GAP.

2.2.1. Synthesis of PECH

1.33 g (0.0144 mol) of butane diol (BDO) in 75 mL methylene chloride was taken in a three necked flask fitted with a thermometer and nitrogen inlet. Seven hundred and fifty microliters of cationic initiator; BF_3-dimethyl ether complex; was injected to the reaction mixture and stirred at room temperature for 30 min. After cooling the reaction vessel to 0 °C using ice-salt mixture, 46.66 g of ECH (0.5044 mol) was added drop by drop (~0.1 mL/min) to the reaction mixture over a period of 12 h. The mole ratio of BDO to ECH is 1:35. Rate of addition was kept as slow as possible to keep the instantaneous concentration of ECH in the reaction mixture very low. At no point of time, the temperature was allowed to go above 0 °C during the reaction.

After the addition of ECH, the reaction was continued for another 4 h at room temperature. Thereafter, the reaction was frozen by adding distilled water. The organic phase containing PECH was extracted into methylene chloride and washed several times with distilled water until neutral to pH. The washed organic phase was dried over sodium sulphate, filtered, and the solvent evaporated off in vacuum at 40 °C to recover 43 g of PECH (89.5% yield).

2.2.2. Synthesis of GAP and preparation of GAP/TEX mixture

Twenty-eight grams of PECH in 100 mL DMF was taken in a three necked flask fitted with a thermometer, nitrogen inlet and water condenser. The reaction mixture was heated to 120 °C, under stirring in an oil bath. Twenty-five grams of sodium azide was added to the mixture and the reaction continued for another 12 h. Thereafter, reaction was frozen by adding distilled water. The unreacted azide and salted out sodium chloride were filtered off. Organic phase containing GAP was extracted to methylene chloride and washed several times with distilled water until neutral to pH. The washed organic phase was dried over sodium sulphate, filtered, and the solvent evaporated off under vacuum. Twenty-three grams of GAP was obtained (82.14% yield).

TEX was synthesized using a novel method developed in our laboratory [15].

A solution of GAP polymer in methylene chloride was mixed with TEX in such a way that the weight ratio of GAP to TEX is maintained at 1:4 in the samples. After mixing, the samples were kept at 60 °C under vacuum to remove the solvent.

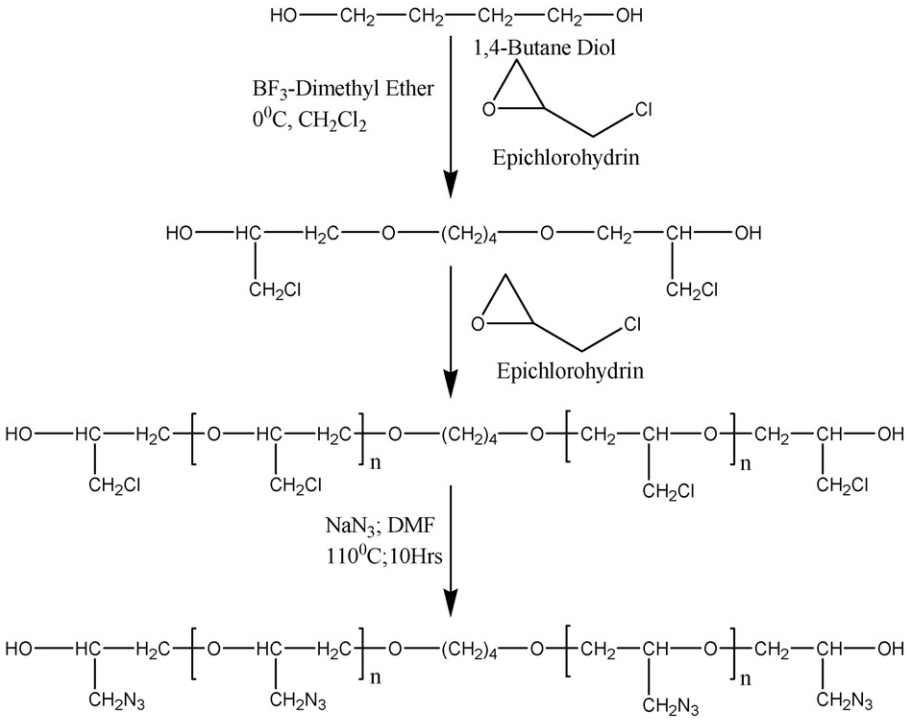

Scheme 1. Synthetic scheme of GAP.

2.2.3. *Instrumental analysis*

GPC analyses of polymers were carried out in a Waters instrument fitted with a 2414 differential refractive index detector against polystyrene standards. ^{1}H NMR spectra was recorded in a Bruker 400 MHz instrument using $CDCl_3$ solvent. FTIR spectra were recorded in a Shimadzu FTIR-8300.

Weight loss measurements were carried out in a Shimadzu TGA-50 thermogravimetric analyzer equipped with thermal analysis software (TA60 Version 1.61) for data analysis. Approximately 5 mg of samples were used for each run. The samples were heated at heating rates of 2.5, 5.0, 7.5, 10, 15 and 20 °C/min in aluminum crucibles under constant flow of nitrogen (50 mL/min). Differential thermo-gravimetric (DTG) curves were obtained after taking the first derivative of TGA curves.

Differential scanning calorimetry (DSC) measurements were carried out in TA Instruments DSC 2010 equipment containing thermal analysis software for data interpretation. In representative runs, 2–3 mg of samples in sealed Aluminum hermetic pans were ramped from room temperature to 320 °C at the rate of 2 °C/min in a steady flow of nitrogen (50 mL/min).

Microscopy observations were done using an Olympus BX-51 microscope fitted with a Linkam THMS 600 hot stage.

2.2.4. *Kinetic analysis of TGA data*

Kinetic analysis of the TGA data was carried out by adopting a model-free method.

2.2.4.1. Model-free method. Model-free methods or iso-conversional methods are based on the principle that reaction rate at a constant extent of conversion is dependent only on the temperature. Model-free methods provide activation energy values that are independent of any implicit reaction model.

We used the model-free method based on Eq. (1) to perform the kinetic analysis [10]:

$$\ln\frac{\beta_i}{T_{\alpha i}^2} = \ln\left[\frac{AR}{E_\alpha g(\alpha)}\right] - \frac{E_\alpha}{RT_{\alpha i}} \qquad (1)$$

where E_α and T_α are activation energy and temperature respectively, for a given value of conversion (α), β the heating rate, A the pre-exponential factor and R is the universal gas constant. Conversion or fractional weight loss is computed as $((W_0 - W_T)/(W_0 - W_\infty))$ where W_0 is the initial weight of the sample, W_T the weight at temperature T, and W_∞ is the final weight of the sample. The samples were heated at multiple heating rates (β_i). Percentage conversions were calculated from the weight loss curves. For each value of conversion, a plot of $\ln[\beta_i/T_{\alpha i}^2]$ versus $1/T_{\alpha i}$ was generated. Activation energy at each value of conversion was calculated from the slope of the generated curves. A computer program was developed in MATLAB [16] for analysis. "Polyfit" function was used to linearly fit $\ln[\beta/T_{\alpha i}^2]$ values with $1/T_{\alpha i}$ at various values of conversion.

3. Results and discussion

3.1. *Synthesis of GAP polymer*

Characterization results of synthesized PECH and GAP polymers are presented in Table 1. The important step in the synthesis of GAP polymer is the synthesis of PECH diol of adequate molecular weight. Usually, for propellant applications, the molecular weight of the prepolymer used as binders is restricted

Table 1
Properties of synthesized polymers

Polymer	Molecular weight[a]	FTIR	^{1}H NMR
PECH	M_w = 2340 kg/mol, M_n = 2018 kg/mol, PDI = 1.16	ν(–OH) = 3450 cm^{-1}, ν(C–O–C) = 1116.7 cm^{-1}, ν(C–Cl) = 746 cm^{-1}	δ = 3.7 ppm (3H; $-CH_2-CH-$), δ = 3.5 ppm (2H; $-CH_2Cl$)
GAP	M_w = 2490 kg/mol, M_n = 2178 kg/mol, PDI = 1.15	ν(–OH) = 3450 cm^{-1}, ν(C–N_3) = 2100 cm^{-1}, ν(C–O–C) = 1100 cm^{-1}	δ = 3.7 ppm (3H; $-CH_2-CH-$), δ = 3.65 ppm (2H; $-CH_2N_3$)

[a] From GPC measurements against polystyrene standards.

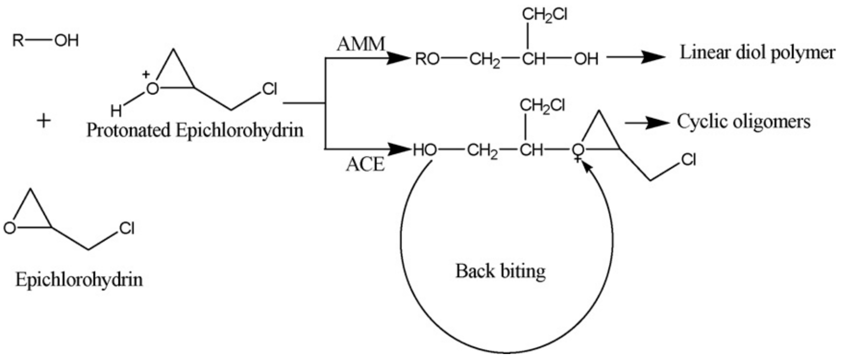

Scheme 2. Illustrations of AMM and ACE mechanisms involved in cationic ring opening polymerizations. AMM produces linear polymers. ACE produces cyclic oligomers by backbiting reactions.

between 2000 and 3000 kg mol^{-1}. This is due to the fact that, higher molecular weight of the prepolymer will lead to higher viscosity incurring high energy costs in processing operations.

Synthesis of PECH takes place by the cationic ring opening polymerization of ECH in the presence of BF_3-dimethyl complex as initiator and BDO as the co-initiator. In cationic ring opening polymerizations, the initiation step is the protonation of the monomer by the initiator. Thereafter, protonated monomer could either react with BDO or the non-protonated monomer. The reaction proceeds through two propagation mechanisms depending on whether the protonated monomer reacts with BDO (activated monomer mechanism (AMM)) or non-protonated monomer (activated chain end mechanism (ACE)) [17]. The quality of the polymer obtained depends on the dominance of one mechanism over the other. The operation of AMM will lead to the formation of the preferred linear diol polymers and the operation of ACE leads to low molecular weight oligomers. These low molecular weight oligomers are mainly constituted of cyclic compounds [18]. Scheme 2 presents the details of the mechanisms of ACE and AMM. From the involved kinetics, in order to enhance the contribution of AMM, the instantaneous concentration of the non-protonated monomer should be kept as low as possible [19].

In this study, we carried out the synthesis of PECH at two different rates of addition of the monomer ECH. The GPC chromatogram of the synthesized polymers is presented in Fig. 2. GPC curve of the polymer synthesized at a slow addition rate of 0.1 mL/min indicates the formation of a high molecular weight polymer (M_n = 2018 g/mol) with less than 5% low molecular weight cyclic compounds. On the other hand, for synthesis carried out at faster addition rates, only low molecular weight cyclic compounds are formed. Thus, controlled addition rate of the monomer is one of the critical parameters to increase the contribution of AMM to the reaction, leading to the formation of high molecular weight linear polymers.

Conversion of PECH to GAP is a straight forward process. It involves nucleophilic substitution of the Chloro group by the Azido group through reacting PECH with sodium azide in DMSO solvent at 110 °C. One hundred percent conversion is achieved by employing a reaction time of 10 h.

3.2. DTG and DSC

Fig. 3(a) presents the DTG traces of GAP, TEX and GAP/TEX mixture, with the respective temperatures. Both GAP

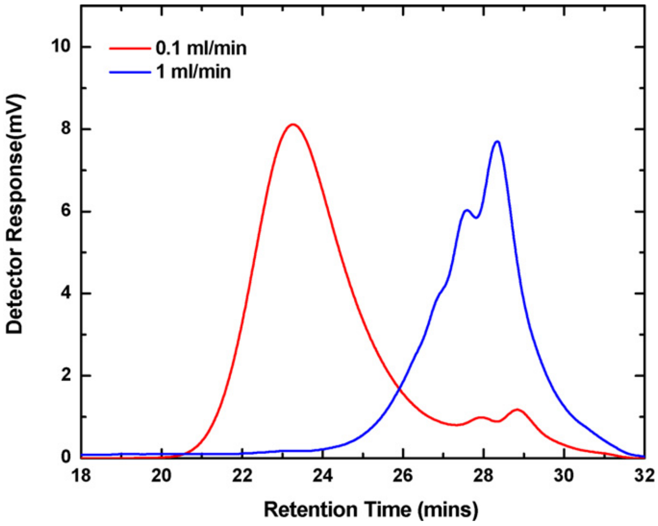

Fig. 2. GPC chromatograms of PECH synthesized at slower and faster addition rates of the monomer. Slower addition rate leads to the formation of low molecular weight oligomers through the predominant operation of ACE mechanism.

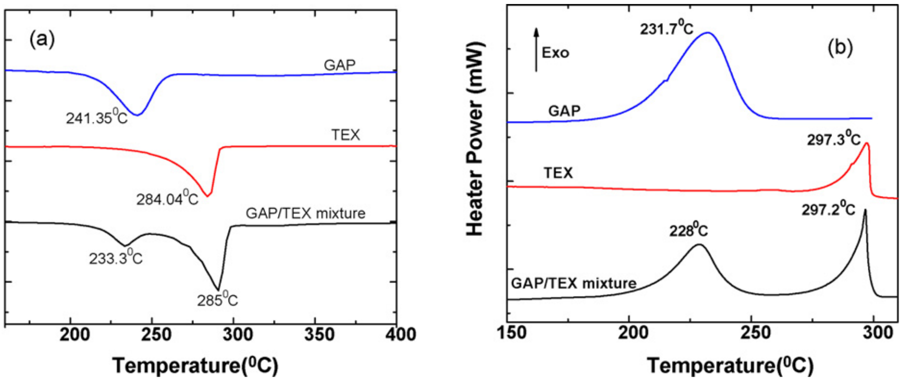

Fig. 3. (a) DTG curves of GAP, TEX and GAP/TEX mixture. The decomposition temperature of TEX does not change in the GAP/TEX mixture. (b) DSC curves of GAP, TEX and GAP/TEX mixture.

and TEX exhibit single DTG peaks at 241.35 °C and 284.04 °C, respectively. The GAP/TEX mixture exhibit double decomposition peaks at 233.3 °C and 285 °C. DSC curves presented in Fig. 3(b) also exhibit consistent results with the DTG curves. The first peak could be ascribed to the decomposition of GAP component in the mixture and the second one to that of TEX.

Some of the previous reports have indicated that the decomposition temperatures of nitramine oxidizers get reduced when they are mixed with polymer binders. Ger et al. [20] reported that, when energetic binders are mixed with RDX and HMX, reduction in the decomposition temperature of the pure constituents takes place. Decomposition of the nitramines in the mixture has been accelerated by the low temperature decomposition of the binder. In another work, Singh et al. [21] have observed reduction in the decomposition temperature of HMX when Estane was coated over it to make plastic bonded explosives (PBX).

In our study, it could be observed from both DTG and DSC curves that the decomposition temperature of TEX does not change when it is mixed with GAP. This means that the decomposition of GAP in GAP/TEX mixture does not affect the decomposition temperature of TEX.

3.3. Thermal decomposition kinetics—model-free approach

GAP thermally decomposes by the exothermic scission of the azide groups to form a nitrene intermediate and nitrogen [22]. The primary mechanism in the decomposition of nitramines is the homolytic fission of N–NO_2 bonds in the molecule [23]. Because the decomposition temperatures of pure GAP and TEX samples are closer to each other, the decomposition of TEX could be catalyzed by the highly exothermic decomposition of GAP. However, we could not observe any shift in the decomposition temperature of TEX in GAP. This means that, there are no molecular level interactions between the components in the mixture and some other mechanistic pathway is determining the thermal decomposition of TEX in the mixture. Therefore, to gain more insights into the mechanistic pathways in the decomposition process, we adopted the model-free method to investigate the kinetics.

Model-free methods reveal the complexity of thermal decomposition process by exhibiting an interdependence of activation energy (E_α) with extent of decomposition. The shapes of the dependence of activation energy with extent of conversion provide information on competing, independent, consecutive, and reversible reactions [24].

Activation energy dependencies were obtained by the linear regressions of the plots of $\ln[\beta_i/T_{\alpha i}^2]$ and $1/T_{\alpha i}$, at different values of conversion, where T_α is the temperature at the given value of conversion derived from the conversion–temperature profiles at various heat rates (β_i). Ninety-five percent confidence intervals for the linear regression were generated and plotted around the regression line. Uncertainties in the activation energy were computed from the differences in slopes of the regression line of the experimental data and that of 95% confidence bands.

Fig. 4 presents the conversion–temperature plots derived from the TGA thermograms of GAP, TEX, and GAP/TEX mixture. GAP shows a gentle variation in conversion with respect to temperature when compared to that of TEX and GAP/TEX mixture. It could be expected that, GAP is having higher activation energy than GAP/TEX mixture or TEX alone. As evident from the DTG/DSC curve, activation energy profile of GAP/TEX

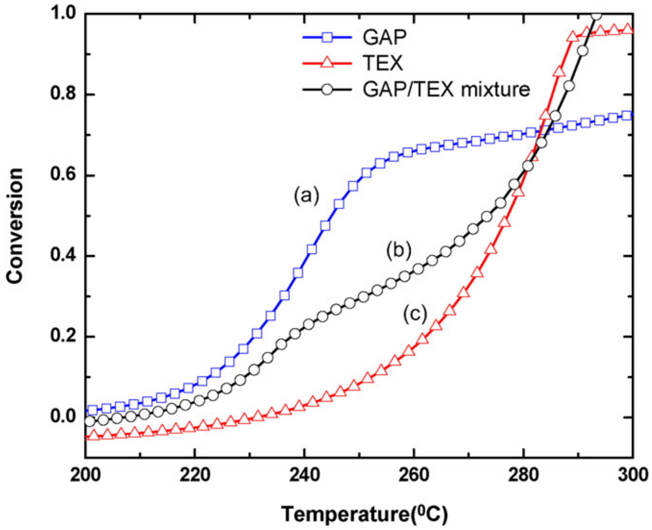

Fig. 4. Representative conversion vs. temperature plots of GAP, TEX and GAP/TEX. These curves were generated from corresponding TGA curves. Heating rate employed was 2 °C/min.

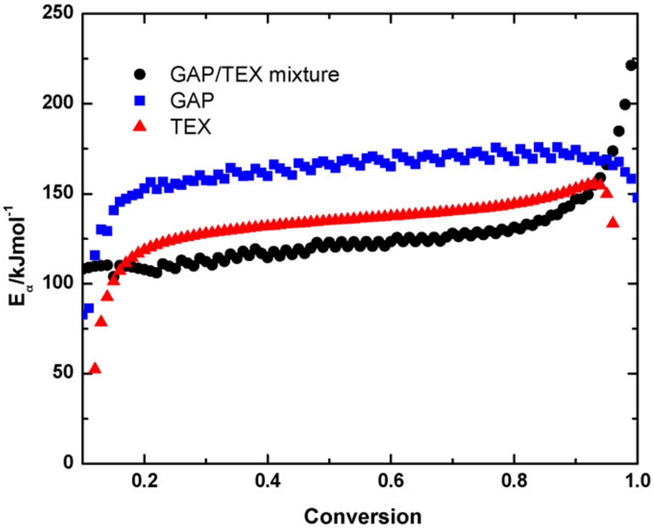

Fig. 5. Dependencies of the activation energy on extent of conversion determined using the model-free isoconversional method for GAP, TEX and GAP/TEX.

mixture exhibit a sight hump at $\alpha = 0.2$. This is due to the decomposition of GAP component in the GAP/TEX mixture. Some changes in the activation energy of thermal decomposition of TEX could be expected when it is mixed with GAP.

The dependencies of activation energy with extent of decomposition for GAP, TEX, and GAP/TEX mixture are presented in Fig. 5. In the thermal decomposition process of GAP, the activation energy increases 82 ± 2 kJ/mol to 145 ± 2 kJ/mol at conversions of $0.1 < \alpha < 0.2$. Then it remains practically independent of extent of decomposition until higher extent of decompositions is reached. The average value of activation energy of thermal decomposition of GAP is 161.7 ± 2 kJ/mol in the conversion range of $0.1 \leq \alpha \leq 1$. This value is consistent with the reported values of activation energy of thermal decomposition for GAP [25]. The activation energy of TEX increases from 50 ± 2 kJ/mol to 125 ± 2 kJ/mol at conversions of $0.1 < \alpha < 0.2$. After $\alpha < 0.2$, the dependence gently increases from 125 ± 2 kJ/mol to 154 ± 7 kJ/mol. At higher conversions of $\alpha < 0.95$ the dependence decreases to 138 ± 10 kJ/mol. The average value of activation energy of thermal decomposition of TEX is 132.7 ± 2 kJ/mol in the conversion range of $0.12 \leq \alpha \leq 0.96$.The value obtained by us is lower than the one predicted by Zeman [26] by means of ^{15}N spectroscopy (213.9 kJ/mol).

Thermal decomposition of materials is accompanied by softening, forming gaseous products inside the decomposing material [27]. The mechanisms controlling this step are either nucleation or nuclei growth. During the initial stages of decomposition process, the concentration of nuclei is very low and the process is limited by nucleation only. With the progress of decomposition, controlling mechanism shifts from nucleation to nuclei growth. Nuclei growth is having a higher activation energy compared to nucleation [28]. This could be the reason for the increasing E_α dependence during the initial stages of decomposition of GAP and TEX. Once initiated, the decomposition process proceeds by the competition of two opposite effects; nuclei growth and nucleation, making the E_α dependence a weak function of conversion [29].

For GAP/TEX mixture, the dependence curve exhibits a decreasing trend from 110 ± 2 kJ/mol to 106 ± 2 kJ/mol in the conversion range of $0.15 \leq \alpha \leq 0.25$. The decrease in activation energy suggests that, another process is competing with solid phase decomposition in this range. Even though the data does not provide any information on the nature of the process, in our case, it could be ascribed to the exothermic decomposition of GAP in the mixture. Thereafter, the dependence gently increases to 160 ± 10 kJ/mol at $\alpha = 0.85$. The average value of activation energy of thermal decomposition of GAP/TEX is 129.75 ± 4 kJ/mol in the conversion range of $0.1 \leq \alpha \leq 0.98$. A literature report [30] on the investigation of decomposition pathways of mixtures of series of nitramines with GAP have pointed out that the presence of GAP-diol decreases the activation energies of certain reaction steps by 20 kJ/mol. It was also predicted that the decompositions of CL-20 and RDX are more easily facilitated in the presence of GAP-diol to a larger extent than the decomposition of HMX. Our investigation also demonstrates that the activation energy of thermal decomposition of GAP/TEX mixture is lower than that of the pure GAP and TEX components. In the absence of any chemical interaction between the components of the GAP/TEX mixture, we assume that the plausible reason for lower activation energy of the mixture is the predominance of mass transfer controlled gas diffusion mechanism [28,31] over the nuclei growth in the mixture.

3.4. Mechanistic aspects of thermal decomposition of GAP/TEX mixture

It is well known that, in uni-molecular energetic materials the decomposition and the corresponding rate of energy release are controlled by chemical kinetics and not by any mass transport mechanisms [32]. On the other hand, in composite energetic materials the reaction kinetics is typically controlled by the diffusion rates between the reactants. In our case, the GAP/TEX mixture could be considered as an energetic composite material and we anticipate that the thermal decomposition of GAP/TEX mixture is controlled by a mass transfer controlled mechanism

We used a combination of optical microscopy (OM) and Fourier transform infrared (FTIR) to investigate the thermal decomposition of GAP/TEX mixture. In the experiment, the mixture was kept on the hot stage of the optical microscope and the mixture was heated at a controlled heating rate of 2 °C/min from room temperature to 300 °C. The morphological changes of the mixture during heating were observed. The residues of the mixture were collected at specific temperatures and FTIR of the residues were taken by dispersing them on KBR pellets. The results are presented in Fig. 6.

At room temperature, FTIR spectra of the mixture exhibits the characteristic peaks due to the azide group (–N_3) stretching in GAP polymer at 2102 cm^{-1} and also the N–NO_2 stretching peak for TEX at 1595.02 cm^{-1}. Upon heating, the GAP component in the mixture decomposes at 238 °C which is evident from the

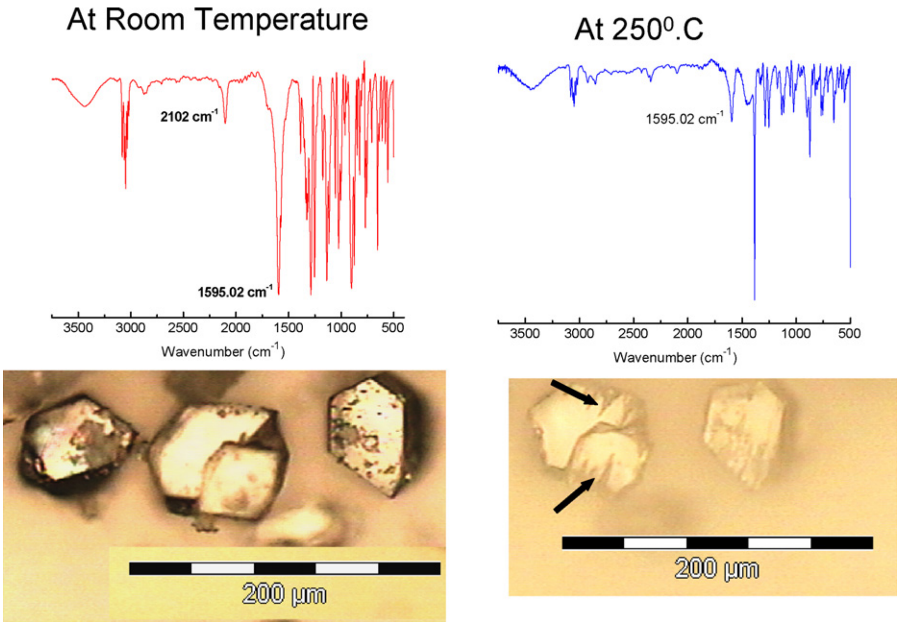

Fig. 6. Comparison of optical micrographs and FTIR spectra of GAP/TEX mixture at room temperature and at 250 °C. The crater like structures formed on the surface of TEX particles is shown as block arrows in the micrograph.

FTIR spectra of the residue collected at 250 °C. The spectra of the residue does not exhibit the peak due to the azide, but the N–NO_2 stretching band of TEX at 1595.02 cm^{-1} is still present. As evident from the DSC/DTG results (Fig. 3), the FTIR result further confirms that the GAP and TEX components decompose independently in the GAP/TEX mixture.

The OM of the mixture at room temperature shows a coating of the GAP polymer on TEX particles. At 250 °C, coating of the GAP polymer on the surface of TEX particles disappears and crater like structures form on the surface of TEX particles. This crater like formations could be the porosity induced by the exothermic decomposition of GAP on the surface of TEX. Similar phenomenon was observed for the decomposition of HMX and the porous morphology has been confirmed by scanning electron microscopy [33]. The porous structure of TEX induced by thermal decomposition of GAP facilitates easy diffusion of the gaseous decomposition by-products of GAP, which facilitates the decomposition of TEX, thereby indicating a plausible operation of a mass-transfer controlled mechanism in the mixture. However, the experimental data presented in this paper is inadequate to eliminate the possibility of the operation of a kinetically controlled process, which warrants a more detailed investigation.

4. Conclusions

This paper describes the synthesis of energetic polymer GAP and thermal decomposition characteristics of its mixture with a high performance nitramine oxidizer TEX. Based on the presented results the following conclusions could be arrived at:

1. Synthesis of GAP polymer was carried out in two stages (Scheme 1). First stage is the synthesis of polyepichlorohydrin (PECH) of adequate molecular weight and the second is the conversion of PECH to GAP through the azidation reaction by sodium azide. PECH was synthesized by the cationic ring opening polymerization of epichlorohydrin (ECH) monomer. It was observed that, a slower rate of addition of ECH is required for the activated monomer mechanism (AMM) to be operative in order to obtain the linear PECH oligomer. Faster addition rates produce low molecular weight cyclic compounds through activated chain end mechanism (ACE).
2. DSC/DTG results indicated that the GAP and TEX components decompose independently in the GAP/TEX mixture. No change was observed for the peak decomposition temperature of TEX in the presence of GAP ruling out any molecular level interaction between the components.
3. Activation energy dependencies obtained from model-free analysis demonstrated that the activation energy of thermal decomposition of GAP/TEX mixture is lower than that of the pure GAP and TEX components. In the absence of any chemical interaction between the components of the GAP/TEX mixture, the predominance of mass-transfer controlled gas diffusion mechanism over the kinetically controlled nuclei growth in the mixture was anticipated. The early stages of degradation of mixture are determined by the thermal decomposition of polymer ($\alpha > 0.25$), whereas the later stages ($0.25 \leq \alpha \leq 1$) are determined by that of TEX.
4. Combination of OM and FTIR were used to deduce mechanistic conclusions for the decomposition of GAP/TEX mixture. It was observed that the decomposition of GAP polymer in the mixture leads to the formation of a porous morphology of TEX. Such a porous structure facilitates easy diffusion of the by-products of the decomposition of GAP, thereby controlling the thermal decomposition of TEX, indicating a plausible operation of a mass-transfer controlled mechanism in the GAP/TEX mixture.

Acknowledgement

The authors acknowledge the financial support from Defense Science and Technology Agency, Singapore for their financial support. Finally, the referee’s constructive comments on the factors affecting thermal decomposition of GAP/TEX have considerably helped to improve the quality of the paper and this is much appreciated.

References

[1] S. Vyazovkin, Anal. Chem. 78 (2006) 3875.
[2] M.B. Frankel, L.R. Grant, J.E. Flanagan, J. Propuls. Power 8 (1992) 560.
[3] N. Kubota, T. Sonobe, A. Yamamato, J. Shimizu, J. Propuls. Power 6 (1990) 686.
[4] M.E. Colclough, H. Desai, R.W. Miller, N.C. Paul, M.J. Stewart, P. Golding, Polym. Adv. Technol. 5 (1994) 554.
[5] K. Karaghiosoff, T.M. Klapotke, A. Michailovski, G. Holl, Acta Cryst. C 58 (2002) 580.
[6] B.D. Roos, T.B. Brill, Propellants Explosives Pyrotechn. 26 (2001) 213.
[7] S. Zeman, Thermochim. Acta 384 (2002) 137.
[8] S. Zeman, M. Dimun, S. Truchilk, Thermochim. Acta 78 (1984) 181.
[9] S. Zeman, Thermochim. Acta 202 (1992) 191.
[10] S. Vyazovkin, C.A. Wight, Thermochim. Acta 340/341 (1999) 53.
[11] J.R. Opfermann, E. Kaisersberger, H.J. Flammersheim, Thermochim. Acta 391 (2002) 119.
[12] S. Vyazovkin, I. Dranca, X. Fan, R. Advincula, Macromol. Rapid Commun. 25 (2004) 498.
[13] R. Mahadevan, D. Lee, H. Sakurai, M.R. Zachariah, J. Phys. Chem. A 106 (2002) 11083.
[14] A. Khawam, D.R. Flanagan, Thermochim. Acta 436 (2005) 101.
[15] D. Bahulayan, H.G. Ang, in: Y.J. Wang, P. Huang, S.C. Li (Eds.), Theory and Practice of Energetic Materials, Science Press, Beijing, 2005, pp. 11–14.
[16] MATLAB Program Manual. http://www.mathworks.com.
[17] P. Kubisa, J. Polym. Sci. (Part A: Polym. Chem.) 41 (2003) 457.
[18] T. Biedron, P. Kubisa, S. Penczek, J. Polym. Sci. (Part A: Polym. Chem.) 29 (1991) 619.
[19] P. Kubisa, S. Penczek, Prog. Polym. Sci. 24 (1999) 1409.
[20] M.D. Ger, W.H. Hwu, C.C. Huang, Thermochim. Acta 224 (1993) 127.
[21] G. Singh, S.P. Felix, P. Soni, Thermochim. Acta 399 (2003) 153.
[22] M.S. Eroglu, O. Guven, J. Appl. Polym. Sci. 61 (1996) 201.
[23] R. Turcotte, M. Vachon, Q.S.M. Kwok, R. Wang, D.E.G. Jones, Thermochim. Acta 433 (2005) 105.
[24] S. Vyazovkin, C.A. Wight, Annu. Rev. Phys. Chem. 48 (1997) 125.
[25] K.V. Puduppakkam, M.W. Beckstead, Combust. Sci. Tech. 177 (2005) 1661.
[26] S. Zeman, Thermochim. Acta 333 (1999) 121.
[27] V. Mamleev, S. Bourbigot, M. Le Bras, S. Duquesne, J. Šesták, Phys. Chem. Chem. Phys. 2 (2000) 4708.
[28] S. Vyazovkin, C.A. Wight, Chem. Mater. 11 (1999) 3386.
[29] B. Saha, A.K. Maiti, A.K. Ghoshal, Thermochim. Acta 444 (2006) 46.
[30] M.A. Bohn, A. Hammerl, K. Harris, T.M. Klapoetke, Centr Eur. J. Energy Mater. 2 (2005) 3.
[31] S. Vyazovkin, Int. J. Chem. Kinet. 28 (1996) 95.
[32] T.M. Tillotson, A.E. Gash, R.L. Simpson, L.W. Hrubesh, J.H. Satcher Jr., J.F. Poco, J. Non-Cryst. Solids 285 (2001) 338.
[33] P. Lofy, C.A. Wight, JANNAF 35th Subcommittee and 17th Propulsion System Hazards Subcommittee Meeting, Joint Sessions, 1998, p. 137.